

AD-A043 319

AEROSPACE CORP EL SEGUNDO CALIF AEROPHYSICS LAB  
SIMPLE MODEL OF A CHAIN-REACTION PULSED HF LASER. (U)  
JUL 77 R L KERBER, J S WHITTIER  
TR-0077(2940)-3

F/G 20/5

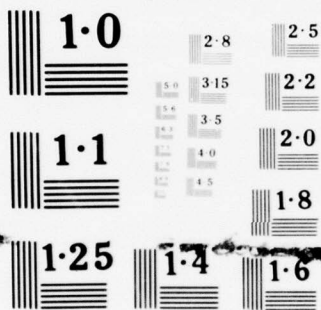
F04701-76-C-0077  
NL

UNCLASSIFIED

SAMSO-TR-77-154

1 OF 1  
ADA  
043319





NATIONAL BUREAU OF STANDARDS  
MICROCOPY RESOLUTION TEST CHART

12

J

AD A 043319

# Simple Model of a Chain-Reaction Pulsed HF Laser

Department of Mechanical Engineering  
Michigan State University  
and  
Aerophysics Laboratory  
The Ivan A. Getting Laboratories  
The Aerospace Corporation  
El Segundo, Calif. 90245

29 July 1977

Interim Report

APPROVED FOR PUBLIC RELEASE;  
DISTRIBUTION UNLIMITED

DDC  
RECEIVED  
AUG 25 1977  
RECEIVED

J

B

Prepared for  
SPACE AND MISSILE SYSTEMS ORGANIZATION  
AIR FORCE SYSTEMS COMMAND  
Los Angeles Air Force Station  
P.O. Box 92960, Worldway Postal Center  
Los Angeles, Calif. 90009

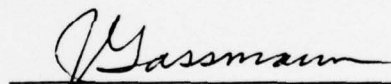
AD No. \_\_\_\_\_  
DDC FILE COPY

This report was submitted by The Aerospace Corporation, El Segundo, CA 90245, under Contract F04701-76-C-0077 with the Space and Missile Systems Organization, Deputy for Advanced Space Programs, P.O. Box 92960, Worldway Postal Center, Los Angeles, CA 90009. It was reviewed and approved for The Aerospace Corporation by W. R. Warren, Jr., Director, Aerophysics Laboratory. Lieutenant A. G. Fernandez, SAMSO/YAPT, was the project officer for Advanced Space Programs.

This report has been reviewed by the Information Office (OI) and is releasable to the National Technical Information Service (NTIS). At NTIS, it will be available to the general public, including foreign nations.

This technical report has been reviewed and is approved for publication. Publication of this report does not constitute Air Force approval of the report's findings or conclusions. It is published only for the exchange and stimulation of ideas.

  
Arturo G. Fernandez, Lt, USAF  
Project Officer

  
Joseph Gassmann, Major, USAF

FOR THE COMMANDER

  
Leonard E. Baltzell, Col, USAF  
Asst. Deputy for Advanced Space  
Programs

UNCLASSIFIED

SECURITY CLASSIFICATION OF THIS PAGE (When Data Entered)

19 REPORT DOCUMENTATION PAGE		READ INSTRUCTIONS BEFORE COMPLETING FORM
18 1. REPORT NUMBER SAMSO-TR-77-154	2. GOVT ACCESSION NO.	3. RECIPIENT'S CATALOG NUMBER
6 4. TITLE (and Subtitle) SIMPLE MODEL OF A CHAIN-REACTION PULSED HF LASER.		5. TYPE OF REPORT & PERIOD COVERED 9 Interim rept.
	14 6. PERFORMING ORG. REPORT NUMBER TR-0077(2940)-3	8. CONTRACT OR GRANT NUMBER(s) 15 F04701-76-C-0077 ✓
10 7. AUTHOR(s) Ronald L. Kerber and James S. Whittier		10. PROGRAM ELEMENT, PROJECT, TASK AREA & WORK UNIT NUMBERS
9. PERFORMING ORGANIZATION NAME AND ADDRESS The Aerospace Corporation El Segundo, Calif. 90245		12. REPORT DATE 11 29 July 1977
11. CONTROLLING OFFICE NAME AND ADDRESS Space and Missile Systems Organization Air Force Systems Command Los Angeles, Calif. 90009		13. NUMBER OF PAGES 36
14. MONITORING AGENCY NAME & ADDRESS (if different from Controlling Office) 12 409 367		15. SECURITY CLASS. (of this report) Unclassified
		15a. DECLASSIFICATION/DOWNGRADING SCHEDULE
16. DISTRIBUTION STATEMENT (of this Report)  Approved for public release; distribution unlimited		
17. DISTRIBUTION STATEMENT (of the abstract entered in Block 20, if different from Report)		
18. SUPPLEMENTARY NOTES		
19. KEY WORDS (Continue on reverse side if necessary and identify by block number)  Pulsed Chemical Laser Chemical Laser Model Chain-Reaction Laser		
20. ABSTRACT (Continue on reverse side if necessary and identify by block number)  With economical, yet accurate, predictions of pulsed $H_2 + F_2$ laser performance as a goal, a rate equation model is formulated that includes only the dominant kinetic mechanisms in the active medium. Effects of model assumptions are examined, and predictions of pulse characteristics are compared with results from a more comprehensive model presented in an earlier study. Computing costs for the present model are less than 1% of those for the comprehensive model; moreover, the present model yields laser pulse → next page		

DD FORM 1473 (FACSIMILE)

UNCLASSIFIED

SECURITY CLASSIFICATION OF THIS PAGE (When Data Entered)

409 367

LB

UNCLASSIFIED

SECURITY CLASSIFICATION OF THIS PAGE(When Data Entered)

19. KEY WORDS (Continued)

20. ABSTRACT (Continued)

characteristics that are consistent with experiment and in excellent agreement with the more comprehensive model. In order to illustrate the model's capability, the effects of initial gas mixture composition and cavity threshold on laser performance are studied over the regime of practical interest. Some possible extensions and applications of the model are also discussed.

UNCLASSIFIED

SECURITY CLASSIFICATION OF THIS PAGE(When Data Entered)

PREFACE

The authors are extremely grateful to M. E. Brennan and J. Lesser for their assistance with the computer calculations.

ACCESSION for	
NTIS	White Section <input checked="" type="checkbox"/>
DDC	Buff Section <input type="checkbox"/>
UNANNOUNCED	<input type="checkbox"/>
JUSTIFICATION _____	
BY _____	
DISTRIBUTION/AVAILABILITY CODES	
Dist.	AVAIL. DATE/CT SPECIAL
A	

CONTENTS

PREFACE .....	1
I. INTRODUCTION .....	5
II. THEORY .....	9
A. Model Formulation .....	9
B. Approximate Model Solution .....	16
C. Comparison with Comprehensive Model .....	19
III. PARAMETRIC STUDY OF LASER PERFORMANCE .....	23
A. Threshold .....	23
B. Initiation Level .....	25
C. Diluents .....	25
D. Initial H <sub>2</sub> Concentration .....	28
E. Initial Temperature .....	28
IV. COMPARISON WITH EXPERIMENT .....	31
V. CONCLUSIONS .....	33
APPENDIX A .....	35
APPENDIX B .....	37
REFERENCES .....	39

## CONTENTS

PREFACE .....	1
I. INTRODUCTION .....	5
II. THEORY .....	9
A. Model Formulation .....	9
B. Approximate Model Solution .....	16
C. Comparison with Comprehensive Model .....	19
III. PARAMETRIC STUDY OF LASER PERFORMANCE .....	23
A. Threshold .....	23
B. Initiation Level .....	25
C. Diluents .....	25
D. Initial H <sub>2</sub> Concentration .....	28
E. Initial Temperature .....	28
IV. COMPARISON WITH EXPERIMENT .....	31
V. CONCLUSIONS .....	33
APPENDIX A .....	35
APPENDIX B .....	37
REFERENCES .....	39

## FIGURES

1.	Comparison of Predicted Power Time Histories for F + H = 0.1 (a), 0.01 (b), and 0.001 (c) . . . . .	20
2.	Effect of Cavity Threshold for Selected Levels of Initiation . . . . .	24
3.	Effect of Level of Initiation for Selected Values of H <sub>2</sub> . . . . .	26
4.	Effect of He Concentration for Selected Values of Initial Pressure . . . . .	27
5.	Effect of H <sub>2</sub> Concentration for Selected Levels of Initiation . . . . .	29
6.	Effect of Initial Temperature at Selected Values of Initial Pressure . . . . .	30
7.	Comparison of Theory and Experimental Results of Hofland et al. <sup>6</sup> at 800 Torr . . . . .	32

## TABLES

I.	Rate Coefficients for H <sub>2</sub> + F <sub>2</sub> Chemical Laser. . . . .	11
II.	Band Energy Level Spacings. . . . .	14
III.	Comparison of Pulse Energy as Predicted by the Simple and the Comprehensive Model. . . . .	22

## I. INTRODUCTION

Interest in  $H_2 + F_2$  chain-reaction pulsed lasers has been increased by steady experimental progress with electrically initiated devices. Electrical efficiencies greater than 100% have been achieved, and large output energies, up to 2360 J, have been achieved in electrically initiated devices.<sup>1-6</sup> These developments have inspired increased interest in modeling of  $H_2 + F_2$  chain lasers for better understanding of performance and for guidance in the design of improved devices. This report presents a simplified rate equation model that, in comparison with earlier models, provides great economy of prediction of laser power and energy with little sacrifice in accuracy. Our model has some ad hoc features. However, we believe this to be amply justified (1) because the  $H_2 + F_2$  laser is of growing importance, and (2) because of the computational economy that is gained.

Modeling of the pulsed  $H_2 + F_2$  laser was pioneered by Emanuel and co-workers.<sup>7-11</sup> Emanuel formulated a "constant-gain" rate equation model that, when solved numerically,<sup>9</sup> provides predictions of instantaneous species concentrations, temperature, and the laser power spectrum of each vibrational band as influenced by rates of chemical pumping and heating, molecular energy transfer and deactivation, dissociation and recombination, and stimulated emission. A study<sup>10</sup> of the sensitivity of model predictions to many parameters was carried out. An early comparison of Emanuel's model with pulsed laser experiments was made by Suchard et al.,<sup>11</sup> who found good agreement with the time-to-laser threshold and pulse shape of their photolytically initiated laser. A related earlier study by Chester and Hess<sup>12</sup> showed good agreement between their photo-initiated experiments and their small-signal-gain rate equation model. More recently, predictions of Emanuel's model have been compared with discharge laser experiments;<sup>13</sup> fair agreement was found for laser power and energy.

Pulsed  $H_2 + F_2$  laser modeling research is progressing along three distinct, but interacting, lines. First, better agreement between model predictions and measured laser power and energy is being sought through kinetic rate adjustments, particularly those of deactivation processes, through incorporation of ionic species in the laser kinetics,<sup>13</sup> as well as through improved experiments. Second, more realistic predictions of laser-output-spectra versus time as well as modest refinements in energy predictions are being sought with models that account for cavity transients and rotational nonequilibrium phenomena.<sup>14-16</sup> The present report belongs to a third line of investigation in which economical predictions are sought of gross laser power and energy through simplification of the comprehensive rate equation approach. It is expected that the paper will contribute to the first two lines of research as follows: The relative importance of various phenomena is clarified in constructing the simple model and in comparing its predictions with those of comprehensive models. Examination of the suitability of proposed rate changes should be facilitated because many parametric combinations can be considered cheaply. For example, theoretical predictions for comparison with the entirety of available laser performance data could easily be repeated for a large number of tentative choices of rate-constant values. Moreover, because of its economy, the model can also be useful as a "building block" in engineering systems analysis studies where laser size, weight, and performance are optimized for specific applications.

Previous work of Skifstad on a simple model for the  $H_2 + F_2$  laser concentrated on the derivation of closed-form analytical results; consequently, for tractability, his analysis assumed constant temperature.<sup>17</sup> In practice, such analytical results usually serve only as a qualitative guide to laser performance as there is generally a large temperature rise during the laser pulse (or downstream in a cw laser). In the present work, we are seeking accurate predictions for a wide range of conditions; hence, we account for temperature variation.

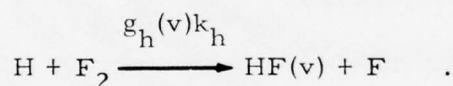
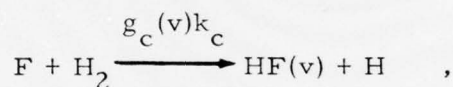
Our analysis (Section II) stems from earlier work on simple models for the DF/CO<sub>2</sub> and F + H<sub>2</sub> pulsed lasers.<sup>18,19</sup> In striving for accurate prediction in the more complicated H<sub>2</sub> + F<sub>2</sub> pulsed laser system, however, we incorporate features that were not included in these earlier studies. The new features are ad hoc methods in which J-shift and lasing cutoff on a particular band are approximated. Model predictions are compared with those of the comprehensive model of Ref. 9. For cases of practical interest, excellent agreement is found. In Section III, the usefulness of the model for parametric variation is illustrated. In Section IV, model predictions are compared with selected experiments.

## II. THEORY

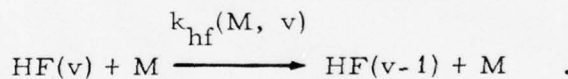
### A. MODEL FORMULATION

A simple model for a pulsed HF laser pumped by the  $H_2 + F_2$  chain reaction is presented. Initially, the medium is assumed to be a homogeneous mixture of  $F_2$ ,  $H_2$ , F, H, and diluent. Relative concentrations of  $F/F_2$  and  $H/H_2$  are chosen to simulate initiation by an external source. The dominant reactions of the chemical system were previously identified<sup>10</sup> as:

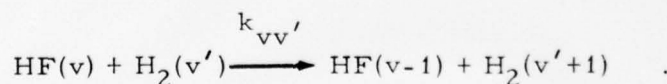
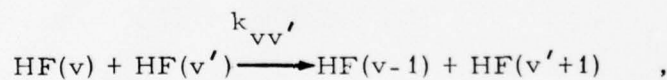
1. The  $H_2 + F_2$  chain:



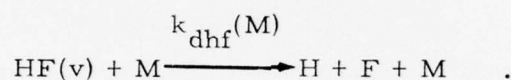
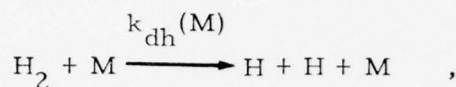
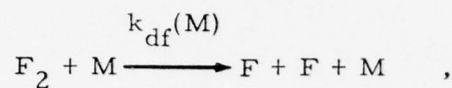
2. Vibration - translation (VT) deactivation:



3. Vibration - vibration (VV) transfer:



4. Dissociation - recombination:



The overall rates of the chain reactions  $k_c$  and  $k_h$  and the fractions of the population produced in the reaction product  $\text{HF}(v)$  given by  $g_c(v)$  and  $g_h(v)$  are easily obtained from the rate coefficients of Reactions (1) and (2) in Table I. For the constant-gain method of solution used in this model, it is known that the effect of the (VV) reactions in item 3 above can be neglected.<sup>10</sup> Initial reactant mixtures with total pressure less than 2 atm are considered; therefore, the dissociation-recombination reactions in item 4 are neglected.

The rate of change of  $\text{HF}(v)$  may be written as<sup>10</sup>

$$\frac{d[\text{HF}(v)]}{dt} = P_v + X_v - X_{v-1} + D_{v+1,v} - D_{v,v-1} \quad , \quad (1a)$$

where chemical pumping is

$$P_v = g_c(v)k_c[\text{F}][\text{H}_2] + g_h(v)k_h[\text{H}][\text{F}_2] \quad , \quad (1b)$$

vibrational deactivation is

$$D_{v,v-1} = [\text{HF}(v)] \sum_M k_{hf}(M, v) [\text{M}] \quad , \quad (1c)$$

and  $X_v$  is the rate of laser photon emission for the band with lower level  $v$ .

Table I. Rate Coefficients for  $H_2 + F_2$  Chemical Laser<sup>a</sup>

Reaction No.	Reaction	Rate Coefficient (cm <sup>3</sup> /mole-sec)	M, v
1a <sup>b</sup>	$F + H_2(0) = HF(1) + H$	$k_{1a} = 2.6 \times 10^{13-1.6/\theta}$	
1b	$F + H_2(0) = HF(2) + H$	$k_{1b} = 8.8 \times 10^{13-1.6/\theta}$	
1c	$F + H_2(0) = HF(3) + H$	$k_{1c} = 4.4 \times 10^{13-1.6/\theta}$	
1d	$F + H_2(0) = HF(4) + H$	$k_{-1d} = 7.4 \times 10^{12-0.50/\theta}$	
1e	$F + H_2(0) = HF(5) + H$	$k_{-1e} = 1.1 \times 10^{13-0.51/\theta}$	
1f	$F + H_2(0) = HF(6) + H$	$k_{-1f} = 1.9 \times 10^{13-0.56/\theta}$	
2a	$H + F_2 = HF(0) + F$	$k_{2a} = 1.1 \times 10^{12-2.4/\theta}$	
2b	$H + F_2 = HF(1) + F$	$k_{2b} = 2.5 \times 10^{12-2.4/\theta}$	
2c	$H + F_2 = HF(2) + F$	$k_{2c} = 3.5 \times 10^{12-2.4/\theta}$	
2d	$H + F_2 = HF(3) + F$	$k_{2d} = 3.6 \times 10^{12-2.4/\theta}$	
2e	$H + F_2 = HF(4) + F$	$k_{2e} = 1.6 \times 10^{13-2.4/\theta}$	
2f	$H + F_2 = HF(5) + F$	$k_{2f} = 3.6 \times 10^{13-2.4/\theta}$	
2g	$H + F_2 = HF(6) + F$	$k_{2g} = 4.8 \times 10^{13-2.4/\theta}$	
2h	$H + F_2 = HF(7) + F$	$k_{2h} = 5.5 \times 10^{12-2.4/\theta}$	
2i	$H + F_2 = HF(8) + F$	$k_{2i} = 2.5 \times 10^{12-2.4/\theta}$	
3a <sub>v</sub> <sup>c</sup>	$HF(v) + M_1 = HF(v-1) + M_1$	$k_{3a_v} = v(10^{14.0-T-0.8} + 10^{0.4-T-3.5})$	$M_1 = HF, v = 1 \dots 8$
3b <sub>f</sub>	$HF(1) + M_2 = HF(0) + M_2$	$k_{3b_f} = 1.5 \times 10^{10-1.1/\theta_T}$	$M_2 = F$
3b <sub>2</sub>	$HF(2) + M_2 = HF(1) + M_2$	$k_{3b_2} = 1.5 \times 10^{10-0.5/\theta_T}$	
3b <sub>v</sub>	$HF(v) + M_2 = HF(v-1) + M_2$	$k_{3b_v} = 1.5 \times 10^{10-T}$	$v = 3 \dots 8$
3c <sub>v</sub>	$HF(v) + M_4 = HF(v-1) + M_4$	$k_{3c_v} = (8 \times 10^{-4} T^4)_v$	$M_4 = F_2, v = 1 \dots 8$
3d <sub>v</sub>	$HF(v) + M_5 = HF(v-1) + M_5$	$k_{3d_v} = v(8.7 \times 10^{-7} T^5)$	$M_5 = He, v = 1 \dots 8$
3e <sub>v</sub>	$HF(v) + M_6 = HF(v) + M_6$	$k_{3e_v} = 1.8 \times 10^{13-0.7/\theta}$	$M_6 = H, v = 1 \dots 8, v^1 < v$
3f <sub>v</sub>	$HF(v) + M_7 = HF(v-1) + M_7$	$k_{3f_v} = v(1 \times 10^5 T^2)$	$M_7 = H_2, v = 1 \dots 8$
4a	$HF(v) + HF(v) = HF(v-1) + HF(v+1)$	$k_{4a} = 1.5 \times 10^{12-T/2}$	$v = 1 \dots 7$
4b	$HF(v) + HF(v+1) = HF(v-1) + HF(v+2)$	$k_{4b} = 0.5k_{4a}$	$v = 1 \dots 6$
4c	$HF(v) + HF(v+2) = HF(v-1) + HF(v+3)$	$k_{4c} = 0.25k_{4a}$	$v = 1 \dots 5$
4d	$HF(v) + HF(v+3) = HF(v-1) + HF(v+4)$	$k_{4d} = 0.125k_{4a}$	$v = 1 \dots 4$
5a	$HF(0) + H_2(1) = HF(1) + H_2(0)$	$k_{5a} = 9 \times 10^{11}$	
5b	$HF(1) + H_2(1) = HF(2) + H_2(0)$	$k_{5b} = 2.9 \times 10^{12}$	
5c	$HF(2) + H_2(1) = HF(3) + H_2(0)$	$k_{5c} = 9 \times 10^{12}$	
5d	$HF(3) + H_2(1) = HF(4) + H_2(0)$	$k_{5d} = 2 \times 10^{13}$	
5e	$HF(0) + H_2(2) = HF(1) + H_2(1)$	$k_{5e} = k_{5a}$	
5f	$HF(1) + H_2(2) = HF(2) + H_2(1)$	$k_{5f} = k_{5b}$	
6a <sub>v</sub>	$H_2(v) + M_8 = H_2(v-1) + M_8$	$k_{6a_v} = v(2.5 \times 10^{-4} T^4)^{4-3}$	$v = 1, 2, M_8 = \text{all except } H, H_2$
7b <sub>v</sub>	$H_2(v) + M_9 = H_2(v-1) + M_9$	$k_{6b_v} = v(10^{-3} T^4)^{4-3}$	$v = 1, 2, M_9 = H, H_2$

<sup>a</sup>Note that dissociation recombination reactions have been neglected.

<sup>b</sup> $\theta = \frac{4.575}{1000} T$  kcal/mole.

<sup>c</sup>M = collision partner, v = vibrational level.

If we assume that the highest level pumped by the chain reaction is HF(N), and that lasing occurs on HF(N)  $\longrightarrow$  HF(N-1) and all lower bands, Eqs. (1) may be solved for  $X_v$  to yield<sup>10</sup>

$$X_v = \sum_{v'=v+1}^N P_{v'} - \sum_{v'=v+1}^N \frac{d[\text{HF}(v')]}{dt} - D_{v+1,v} \quad (2)$$

The total rate of increase in the HF(v) population is related to the pumping rate by

$$\sum_{v=0}^N \frac{d[\text{HF}(v)]}{dt} = \sum_{v=0}^N P_v \quad (3a)$$

The integral of this relation may be stated as (at time t)

$$\sum_{v=0}^N \text{HF}(v) = 2 \{ [\text{H}_2]_{t=0} - [\text{H}_2]_t \} \quad (3b)$$

The total rate of photon emission is given by

$$X_T = \sum_{v=0}^{N-1} X_v \quad (4)$$

Therefore,

$$X_T = \sum_{v=1}^N P_v - \sum_{v=1}^N \frac{d[\text{HF}(v)]}{dt} - \sum_{v=0}^{N-1} D_{v+1,v} \quad (5)$$

During lasing, we assume that the gain at line center for the transition lasing in each band is maintained at the cavity threshold value  $\alpha_{\text{thr}}$

$$\alpha_{\text{thr}} = -\frac{1}{2L} \ln(R_O R_L) \quad , \quad (6)$$

where  $L$  is the length of the active medium,  $R_O$  is the reflectivity of the output coupler, and  $R_L$  accounts for a combination of the reflectivity of the second mirror and other cavity losses. The gain at line center on the P-branch of the transition with lower level  $J$  is

$$\alpha(v, J) = \frac{hN_A}{4\pi} \omega(v, J) \phi(v, J) B_{vJ} \left[ \frac{(2J+1)}{2J-1} \text{HF}(v+1, J-1) - \text{HF}(v, J) \right] \quad , \quad (7)$$

where  $N_A$  is Avogadro's number,  $h$  is Planck's constant,  $\omega(v, J)$  is the wavenumber of the transition,  $\phi(v, J)$  is the Voigt line shape function evaluated at line center (Appendix B), and the Einstein isotropic absorption coefficient is  $B_{vJ} = 6.2828 \times 10^{50} |M_{v+1,v}|^2 J/(2J+1)$ ,  $\text{cm}^2/\text{molecule} \cdot \text{J} \cdot \text{sec}^8$ . We approximate the electric dipole matrix element by<sup>8</sup>

$$M_{v+1,v} = (v+1)^{1/2} \times [0.988 \times 10^{-19} \times (1 + 2.66 \times 10^{-2} J)] \quad . \quad (8)$$

The value of  $\omega(v, J)$  is taken as<sup>8</sup>

$$\omega(v, J) = \omega_v - \frac{60.32}{1.4388} J \quad , \quad (9)$$

where the  $\omega_v$  used are given in Table II.

A Boltzmann distribution of the rotational levels is assumed, and translational and rotational degrees of freedom are taken to be in equilibrium; therefore,

$$\text{HF}(v, J) = \text{HF}(v) \frac{\theta_r(v)}{T} (2J+1) \exp[-J(J+1) \theta_r(v)/T] \quad , \quad (10)$$

Table II. Band Energy Level Spacings

Transition (v+1), v	$\omega_v$ (cm <sup>-1</sup> )
1,0	3950
2,1	3790
3,2	3630
4,3	3470
5,4	3320
6,5	3170
7,6	3020
8,7	2880
9,8	2730

where  $\theta_r(v)$  is approximated by<sup>20</sup>

$$\theta_r(v) = (30 - v)K \quad . \quad (11)$$

Because  $\alpha(v, J) = \alpha_{thr}$  during lasing on the  $v+1 \rightarrow v$  band, Eq. (10) may be substituted into (7) to determine a relationship between populations in the levels of lasing bands. Therefore, during lasing, the concentrations satisfy the relation

$$HF(v+1) = z(v, J) + HF(v) \eta_J(v) \quad , \quad (12a)$$

where

$$z(v, J) = \frac{4\pi T \alpha_{thr} \gamma_{v+1}^{J(J-1)}}{h N_A \omega(v, J) \phi(v, J) B_{vJ} \theta_r(v+1) (2J+1)} \quad , \quad (12b)$$

and

$$\eta_J(v) = \frac{\theta_r(v)}{\theta_r(v+1)} \frac{\gamma_{v+1}^{J(J-1)}}{\gamma_v^{J(J+1)}} \quad , \quad (12c)$$

and

$$\gamma_v = e^{\theta_r(v)/T} \quad . \quad (12d)$$

The time history of the temperature may be determined from the energy equation

$$\sum_i [N_i] C_{v_i} \frac{dT}{dt} = -P_L - \sum_i \frac{d[N_i]}{dt} H_i \quad , \quad (13)$$

where  $H_i$  is the molar enthalpy,  $C_{v_i}$  is the molar specific heat at constant volume of species  $i$ , and  $P_L$  is the laser power per unit volume defined by

$$P_L = hc N_A \sum_{v=0}^{N-1} \omega(v, J) X_v \quad . \quad (14)$$

## B. APPROXIMATE MODEL SOLUTION

An approximate method for solution of the model equations is discussed. This method incorporates various physical approximations to facilitate solution by simple numerical computation. Recall that we have already included the following approximations:

1. The mixture is assumed homogeneous, and initiation is simulated by introducing an initial F and H atom concentration.
2. During lasing, the gain at line center is maintained at the threshold value.
3. Vibration-vibration relaxation mechanisms may be neglected.
4. The rotational levels are in equilibrium.
5. Reverse reactions may be neglected.

In order to obtain a simple, but useful, solution, some additional assumptions and approximations are made. With operation of the chain, the rate of change of the F-atom concentration is given by

$$\frac{d[F]}{dt} = [H] [F_2] k_h - [F] [H_2] k_c \quad , \quad (15)$$

and the simple relation between the chain carriers gives

$$[F + H]_t = [F + H]_{t=0} \quad . \quad (16)$$

From earlier work,<sup>10</sup> it is known that the ratio  $[F]/[H]$  quickly assumes a value given by the steady-state chain condition

$$[F] [H_2] k_c \approx [H] [F_2] k_h \quad . \quad (17)$$

Because this ratio is approached on a time scale that is short in comparison with the laser pulse length, we assume that Eq. (17) holds for all time. These approximations permit simplification of Eq. (1b) to

$$P_v = G_v k_c [F] [H_2] \quad , \quad (18a)$$

where

$$G_v = g_c(v) + g_h(v) \quad . \quad (18b)$$

By approximating the heat released to be that of the chain, Eq. (13) becomes

$$\sum_i [N_i] C_{v_i} \frac{dT}{dt} \approx [F] [H_2] k_c \Delta H - P_L - h_\ell \sum_v \frac{d[HF(v)]}{dt} \quad , \quad (19)$$

where  $\Delta H$  is 129.6 kcal/mole, and  $h_\ell$  is taken to be 11.0 kcal/mole.

The number of monatomic and diatomic molecules is not changed by the reaction; therefore, we assume that the specific heat at constant volume of the mixture is constant and equal to its initial value.

To facilitate determination of approximate  $HF(v)$  concentrations, we further assume that (1) the lasing bands terminate in sequence with the 1-0 band shutting off first and that (2) all bands are lasing on transitions that have the same value of  $J$ . Termination is assumed to occur when  $X_v$ , as given in Eq. (2), first becomes negative. Previous studies with the comprehensive model of Emanuel indicated that the 1-0 band shuts off first in the pulse, whereas the other bands shut off nearly simultaneously at some later

time, or those that lase for longer times do so at greatly reduced intensities.<sup>10</sup> Hence, essentially all higher bands terminate at nearly the same time and at a time somewhat later than for the 1-0 band. This behavior is accurately predicted by assumption (1) and our somewhat ad hoc definition of termination.

One cannot expect a gain-equals-loss model to predict time-resolved spectra such as given by Hough and Kerber.<sup>14</sup> Therefore, the second assumption (2) that all transitions lase on the same value of J is not a severe one. However, the fact that this J must shift during the run in order to predict accurate results is significant. We assume a value of J that maximizes the population of the lower level of the lowest lasing band. This implies that the excited HF population approaches the minimum necessary to maintain lasing on these bands. This result is linked to the constant-gain assumption and is, in fact, compatible with it. Typically, the J values that occur are between 2 and 17. This J-shift is necessary for the calculations to yield time histories of HF(v) that are comparable with those of the comprehensive model.

These assumptions lead to some notation simplifications; for example, we let

$$z_v = z(v, J) \quad , \quad (20)$$

and similar definitions for  $\gamma_v$ ,  $\omega_v$ ,  $\phi_v$ , and  $B_v$  are made. Therefore, Eq. (12b) takes the form

$$z_v = \frac{4\pi T\alpha_{\text{thr}} \gamma_{v+1}^{J(J-1)}}{hN \frac{\omega_v \phi_v B_v \hat{\theta}_r}{A_v} (v+1) (2J+1)} \quad , \quad (21)$$

and Eq. (11a), which relates populations associated with lasing bands, becomes

$$\text{HF}(v+1) = z_v + \text{HF}(v)\eta_v \quad . \quad (22)$$

If we denote by  $v^*$  the lower level of the lowest band lasing at a given time, we can write the rate of change of the nonlasing HF(v) populations as

$$\frac{d}{dt} \sum_{v=0}^{v^*-1} HF(v) = \sum_{v=0}^{v^*-1} P_v + D_{v^*, v^*-1} \quad (23)$$

From Eq. (22), which holds for  $v \geq v^*$ , we can show that

$$\begin{aligned} \sum_{v=v^*}^N HF(v) &= \sum_{v=v^*}^{N-1} z_v + HF(v^*) \left( 1 + \sum_{v=v^*}^{N-1} \prod_{v'=v^*}^v \eta_{v'} \right) \\ &\quad + \sum_{v=v^*}^{N-2} z_v \sum_{v'=v}^{N-2} \prod_{v''=v'+1}^{N-1} \eta_{v''} \end{aligned} \quad (24)$$

The integral of Eq. (23), when summed with Eq. (24), gives the sum of HF(v) over all v, which is also given by Eq. (3b).

Therefore, we can determine HF(v\*) as given in Eq. (24) by combining these relations. The preceding equations can be solved numerically for the time histories of HF(v), T,  $X_v$ , etc. provided that a value for J is specified. (We use a simple forward difference routine.) At each integration step, we choose the value of J that makes HF(v\*) a maximum. This population is normally driven to a maximum as a result of stimulated emission from radiation fields.

### C. COMPARISON WITH COMPREHENSIVE MODEL

In Fig. 1, time histories of intensity for various levels of initiation are compared with the predictions of the comprehensive model of Emanuel

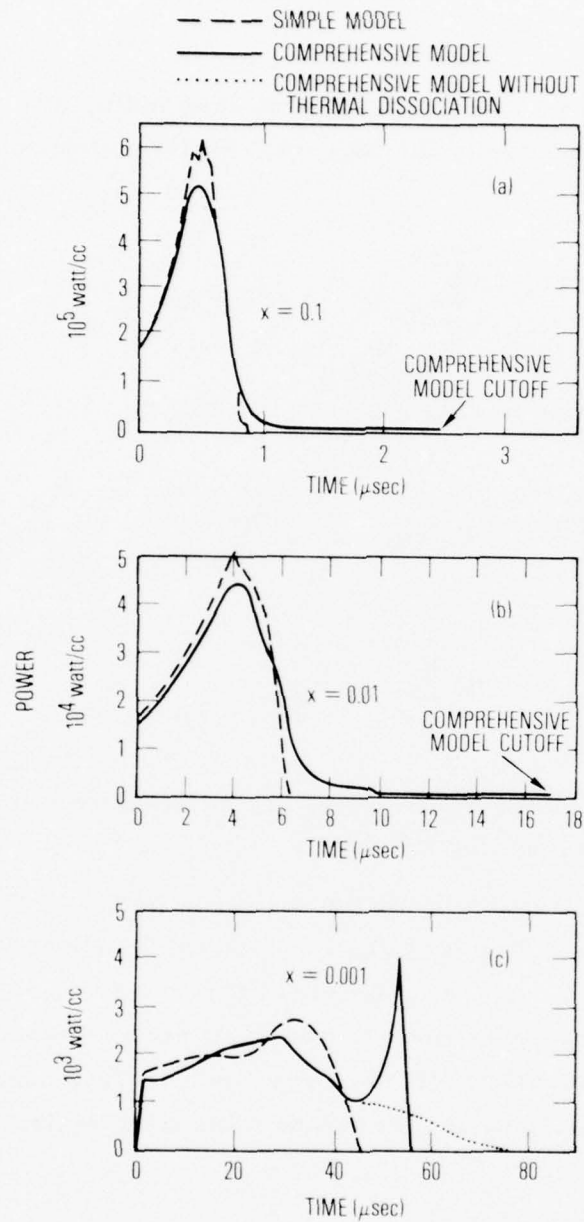


Figure 1. Comparison of Predicted Power Time Histories for  $F + H = 0.1$  (a),  $0.01$  (b), and  $0.001$  (c). Initial gas mixture:  $F + H : H_2 : F_2 : He, F + H : 1 : 1 : 20; 2$   
 $T_i = 300 \text{ K}, P_i = 1 \text{ atm};$   
 cavity conditions:  $R_O = 0.9, R_L = 1.0, L = 100 \text{ cm}.$

et al.<sup>9-11</sup> The figure shows that our model does quite well for  $[F + H]/[F_2] = 0.1$  and  $0.01$ . However, for  $[F + H]/[F_2] = 0.001$ , we find that the simple model is somewhat low, and that the comprehensive model gives a surprising result. The spike near the end of the calculation with the comprehensive model was caused by production of F atoms from thermal dissociation owing to the increase in temperature. This phenomenon, which is dependent on the bond strength of  $F_2$ , should be viewed with some skepticism until experimental corroboration is obtained. Since the present model does not include thermal dissociation, a second calculation with the comprehensive model was made that neglected  $F_2$  dissociation [dotted curve of Fig. 1(c)]. With dissociation suppressed, the agreement between the models is greatly improved. As stated earlier, the primary goal of this work is to develop an efficient method of predicting pulse energy and time histories of pulse intensity. We find, from Fig. 1, that the predicted intensities are closely approximated except near pulse termination. At termination, the simple model predicts a more abrupt shutoff than the more extensive calculations indicate. However, the cutoff time of the simple model is an excellent indication of the time to release most of the pulse energy. Pulse energies for the two models are compared in Table III. Over the wide range of initiation levels considered, the pulse energies from the two models agree to within 5%.

The step-size sensitivity of the simple model was examined by varying the number of steps used in determining the time history of  $HF(v)$  between 100 and 1000. The answers varied by less than 3% for most cases studied. The computational time of the simple model is approximately 1.0 to 1.3% of the comprehensive model. In fact, all 200 simple-model calculations carried out in this study were performed with less computer time than was required for two typical cases with the comprehensive model.

Table III. Comparison of Pulse Energy as Predicted by the Simple and the Comprehensive Model

[F+H]/[F <sub>2</sub> ]	Comprehensive Model	Simple Model
	Pulse Energy (J/liter)	
0.1	291	306
0.01	208	205
0.001	103 (100) <sup>a</sup>	100

<sup>a</sup> Calculation with dissociation of F<sub>2</sub> suppressed.

### III. PARAMETRIC STUDY OF LASER PERFORMANCE

In this section, the effect of varying the initial gas mixture and cavity conditions is examined. The laser pulse is characterized by its duration  $t_c$ , peak power  $P_p$ , and total energy  $E$ . The variations are made about a standard case with 1 F<sub>2</sub>:1 H<sub>2</sub>:0.01 (H+F):20 He with  $T_i$  equal to 300 K and  $P_i$  equal to 1 atm. The standard cavity conditions have  $R_O$ ,  $R_L$ , and  $L$  equal to 0.9, 1.0, and 100 cm, respectively. For brevity, only in Fig. 2 do we include results for peak power  $P_p$  and the time at which it occurs  $t_p$ .

#### A. THRESHOLD

As expected, we find that  $E$  and  $t_c$  increase with decreasing cavity losses. These trends are shown in Fig. 2. The agreement between the two models on the prediction of pulse energy is very good for the case  $[F+H]/[F_2] = 0.01$ . Also shown in Fig. 2(a) is a family of curves obtained from the simple model for several different levels of initiation. The predictions of  $P_p$  also compare favorably with the comprehensive model shown in Fig. 2(c). As shown in Fig. 2(b), the two models agree very well on predictions of  $t_p$ ; however, the agreement of values of  $t_c$  are poorer. (This result is also shown in Fig. 1.) This is because the comprehensive model tends to yield pulses with long low power tails, whereas, the simple model shows a more abrupt cutoff. Except for this discrepancy, the models are found to agree very well. The behavior observed here is similar to that observed earlier for the effect of cavity loss on all pulse characteristics. As expected, the laser performance is more sensitive to cavity threshold for low levels of initiation [Fig. 2(a)]. This may be noted by observing the change in the character of the curve for  $X = 10^{-4}$ .

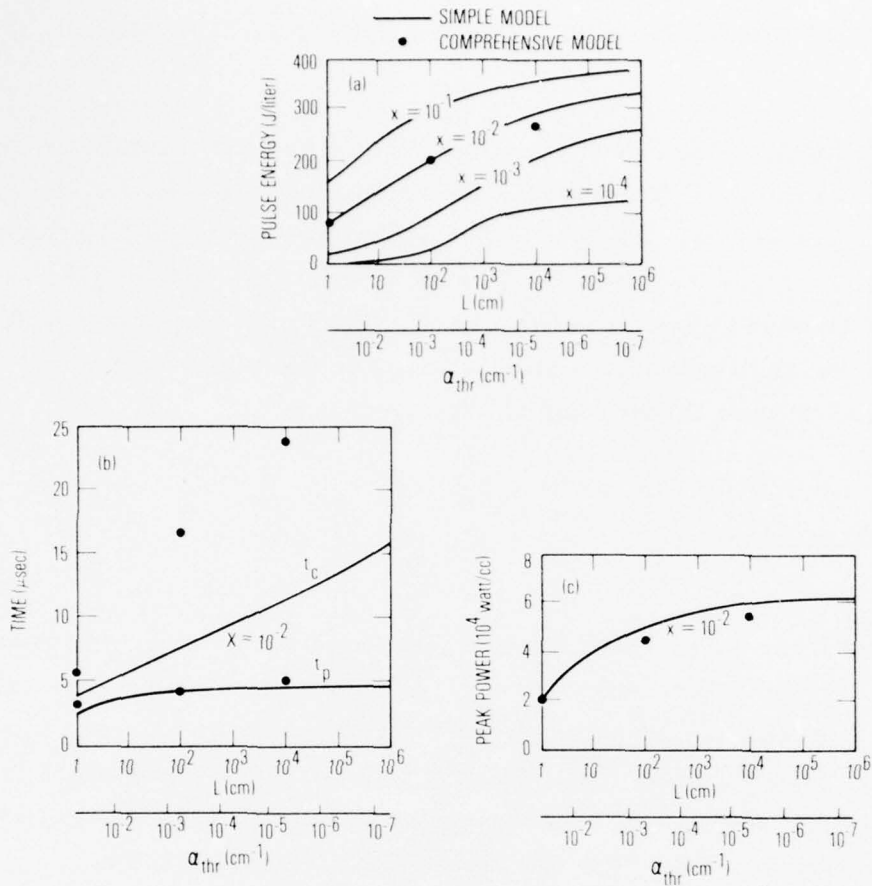


Figure 2. Effect of Cavity Threshold for Selected Levels of Initiation. a. Effect on pulse energy. b. Effect on characteristic times. c. Effect on peak power. Initial gas mixture: F + H : H<sub>2</sub> : F<sub>2</sub> : He, X : 1 : 1 : 20; T<sub>i</sub> = 300 K, P<sub>i</sub> = 1 atm; cavity conditions: R<sub>O</sub> = 0.9, R<sub>L</sub> = 1.0.

## B. INITIATION LEVEL

The initial atom concentration was varied while all other conditions were held fixed. Again, the behavior predicted is very similar to that found earlier,<sup>10</sup> except that we are able to examine efficiently the behavior at very low levels of initiation with the simple model. The results are shown in Fig. 3. The decrease in  $t_c$  and the change in slope in the curve for E as  $[F+H]/[F_2]$  decreases below  $10^{-4}$  reflect the sensitivity of long-chain systems to cavity losses (threshold). The agreement between the comprehensive model and the simple model in predicting E over a wide range is very good [Fig. 3(a)]. The times used for the comprehensive model in Fig. 3(b) are the times at which the power has dropped to 10% of its peak value. Examination of Fig. 1 shows that this is a better indicator of pulse length than is  $t_c$ . It was desired to compare with the comprehensive model at even lower values of  $[F+H]/[F_2]$ ; however, the computations with it became prohibitively long in that regime.

## C. DILUENTS

In Fig. 4, the effect of varying the helium diluent concentration is examined for several initial mixture pressures. Here, as the diluent is increased, reactants decrease because total pressure is held constant. The results are consistent with our expectation that increased diluent at the expense of reactants would yield lower energies. Also, longer pulse lengths result because of lower reactant pressures and temperature. The dashed curves illustrate the effect of diluent on pulse characteristics for mixtures of constant reactant concentration. Since the VT deactivation rate by He is small compared with that of HF by itself, this result is primarily an effect of temperature control. Again, the agreement is excellent between the two models on the predicted pulse energy.

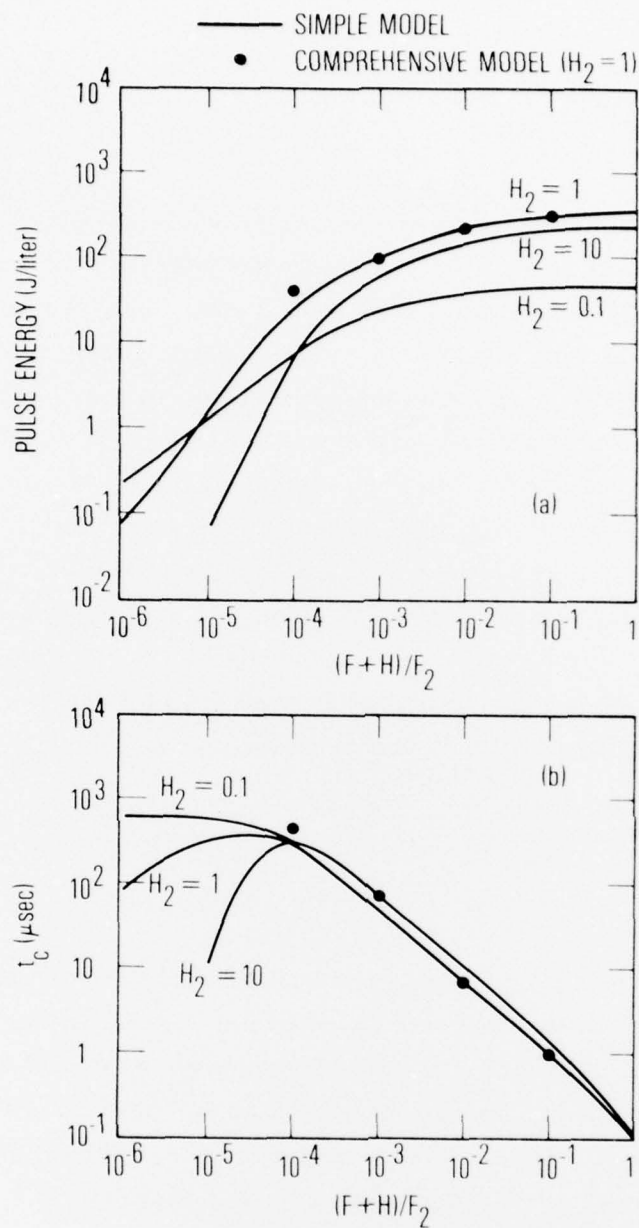


Figure 3. Effect of Level of Initiation for Selected Values of  $H_2$ . a. Effect on pulse energy. b. Effect on pulse duration. Initial gas mixture:  $F + H : H_2 : F_2 : He, X : 1 : 1 : 20$ ;  $T_i = 300 \text{ K}$ ,  $P_i = 1 \text{ atm}$ ; cavity conditions:  $R_O = 0.9$ ,  $R_L = 1.0$ ,  $L = 100 \text{ cm}$ .

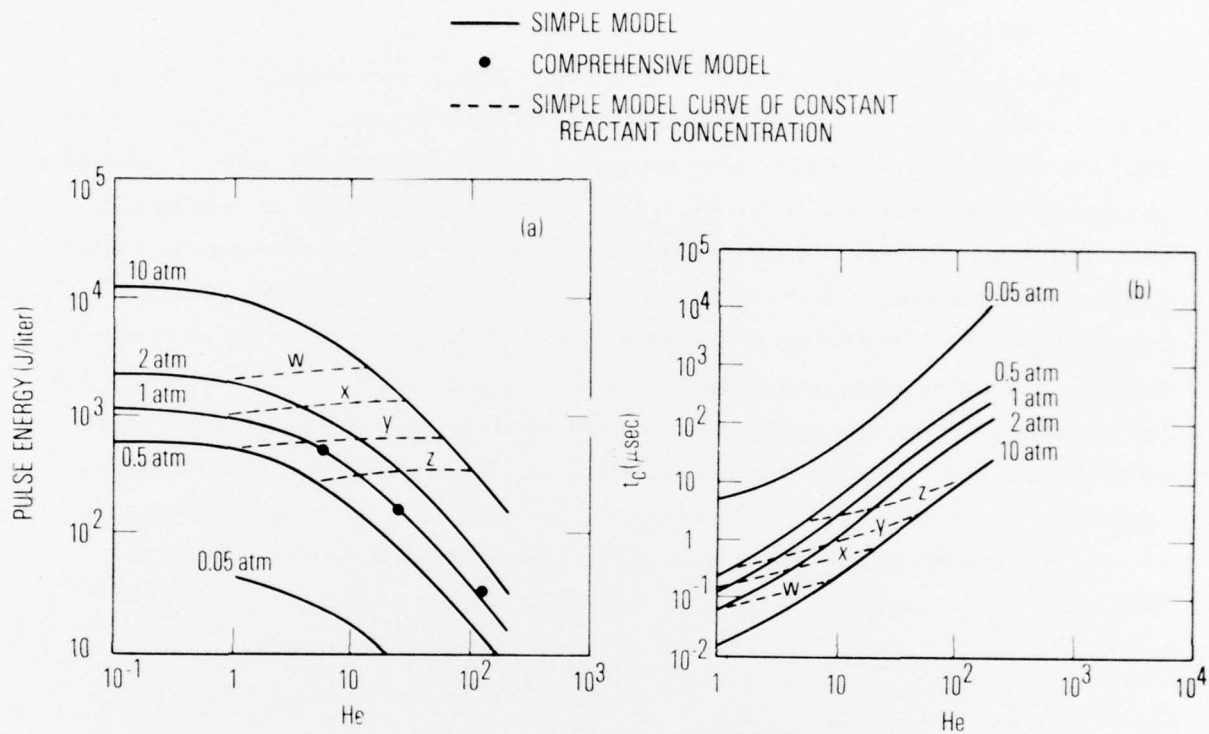


Figure 4. Effect of He Concentration for Selected Values of Initial Pressure. The dashed curves represent loci of constant reactant concentration. Curves w, x, y, and z represent  $F_2$  concentrations of 505, 252, 126, and 54 Torr, respectively. a. Effect on pulse energy. b. Effect on pulse duration. Initial gas mixture: F + H :  $H_2$  :  $F_2$  : He, 0.01 : 1 : 1 : He;  $T_i = 300$  K; cavity conditions:  $R_O = 0.9$ ,  $R_L = 1.0$ ,  $L = 100$  cm.

#### D. INITIAL H<sub>2</sub> CONCENTRATION

The initial [H<sub>2</sub>] was varied while other conditions were the same as those for the standard case for typical levels of initiation. The pulse energy shows a maximum, and the pulse duration shows a minimum when the mixture is nearly stoichiometric (Fig. 5). The behavior as [H<sub>2</sub>] increases to the stoichiometric mixture is clear; more reactant increases the reaction speed and energy released. For mixtures significantly above stoichiometric, we find that [H<sub>2</sub>] is increasing at the expense of [F<sub>2</sub>]; therefore, we observe a decrease in pulse energy and an increase in pulse duration. The curves are fairly flat in the region just above stoichiometric, which indicates a very weak dependence of pulse characteristics on [H<sub>2</sub>] in this region. This behavior is observed over a wide range of initiation levels (Fig. 3). Again, the simple model yields pulse energies in excellent agreement with the comprehensive model.

#### E. INITIAL TEMPERATURE

The initial gas mixture concentration is inversely proportional to the initial temperature for a constant pressure system. Therefore, the behavior seen in Fig. 6 is caused mainly by the amount of reactants available to generate laser energy. Recall that the rate coefficients for all reactions are less well known below 300 K, and predictions in this regime may be suspect.

The disagreement between the two models observed in Fig. 6(a) is the greatest found in the entire study. Above 400 K, the two models begin to differ considerably. However, this does not appear to be a severe problem as it is not anticipated that any useful system will be initiated at elevated temperatures.

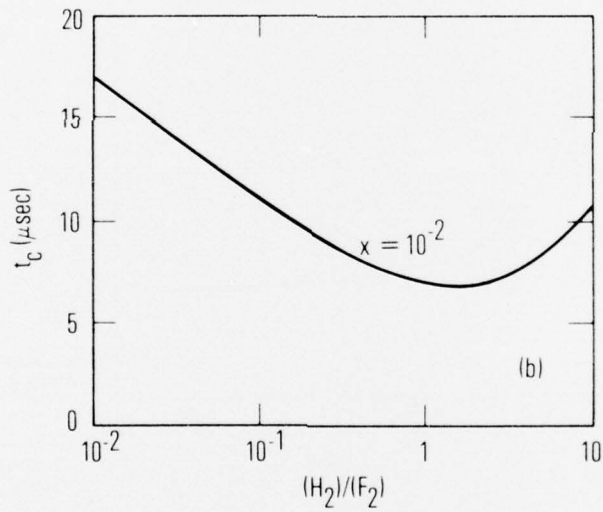
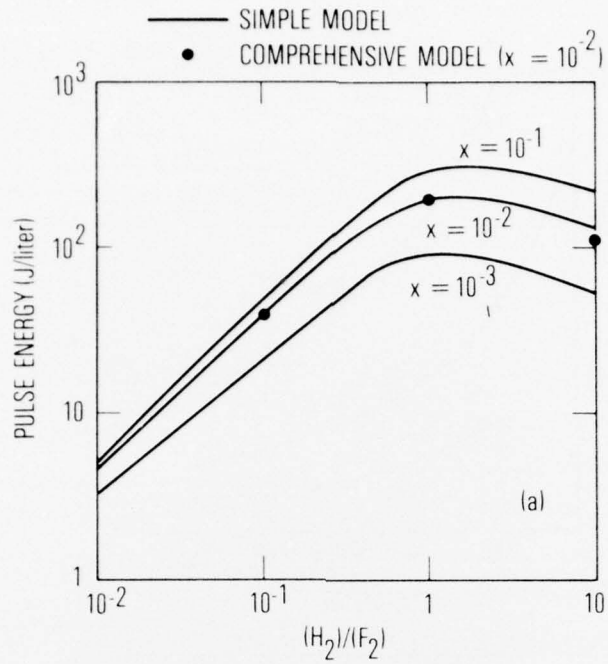


Figure 5. Effect of  $H_2$  Concentration for Selected Levels of Initiation. a. Effect on pulse energy. b. Effect on pulse duration. Initial gas mixture:  $F + H : H_2 : F_2 : He, X : H_2 : 1 : 20$ ;  $T_i = 300$  K,  $P_i = 1$  atm; cavity conditions:  $R_O = 0.9$ ,  $R_L = 1.0$ ,  $L = 100$  cm.

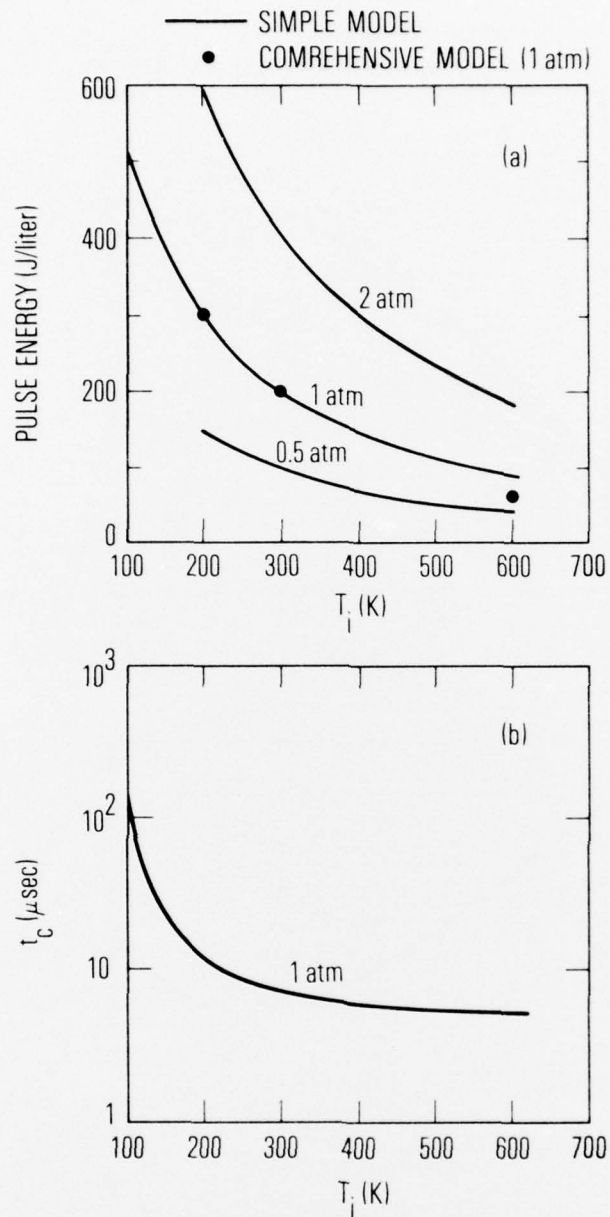


Figure 6. Effect of Initial Temperature at Selected Values of Initial Pressure. a. Effect on pulse energy. b. Effect on pulse duration. Initial gas mixture: F + H : H<sub>2</sub> : F<sub>2</sub> : He, 0.01 : 1 : 1 : 20; cavity conditions: R<sub>O</sub> = 0.9, R<sub>L</sub> = 1.0, L = 100 cm.

#### IV. COMPARISON WITH EXPERIMENT

Since this model has been found to be equivalent to the comprehensive model over the wide region of interest for most practical lasers, its ability to predict energy and power of experimental devices is comparable with that of the comprehensive model.

We have used the model in an effort to predict the experimental results obtained by Hofland et al.<sup>6</sup> First, the model was compared with experiment by using the rate coefficients listed in Table I. The value of  $[F + H]/[F_2]$  was selected by matching pulse energies at a selected value of  $H_2$  concentration. The estimated  $[F + H]/[F_2]$  ratio was 0.005 for cases with argon and 0.003 for cases without argon. Although the predicted energy followed that of experiment quite well for variations in  $[H_2]$ , the predicted pulse duration was about six times longer than observed in the experiment. The value of  $[F + H]/[F_2]$  was also estimated to be 0.06 by matching pulse durations. The calculated pulse energies were then roughly a factor of 4 larger than observed experimentally.

Finally, the rate coefficient for HF-HF V-T relaxation was assumed to be of the form

$$k_{3_{av}} = v^{2.4} k_{3_{a1}}$$

as suggested by the recent results of Kwok.<sup>21</sup> In Fig. 7, calculations using our model and this rate are compared with experiment. The conditions of the experiments are listed in the figures. An additional loss of 10% was assumed to account for contingencies such as volume and surface scattering losses. The value for  $[F + H]/[F_2]$  was determined by matching the pulse energies at  $H_2 = 3$ . For the mixtures without argon,  $[F + H]/[F_2]$  was 0.005, and for mixtures with argon  $[F + H]/[F_2]$  was 0.009 and 0.006 for cases with

[He] = 36 and 54, respectively. On doing this, we found that the model predicts pulse durations within 10% of those observed experimentally.

Although we expected discrepancies between experiment and theory, we emphasize them to illustrate the need for the simple model. The simple model may be used (1) to test efficiently the sensitivity to rate coefficient variations, and (2) to incorporate efficiently the effects of plasma kinetics or mode structure. If, after such modifications, this model begins to compare favorably with experiment, we can then return justifiably to the more expensive comprehensive calculations.

SYM	F <sub>2</sub>	H <sub>2</sub>	He	Ar	E (kV/cm)	C <sub>op</sub> (%)
△	4	X	96-X	0	8.25	10
○	4	X	36	60-X	10	20
□	6	X	54	40-X	11.5-12.5	20

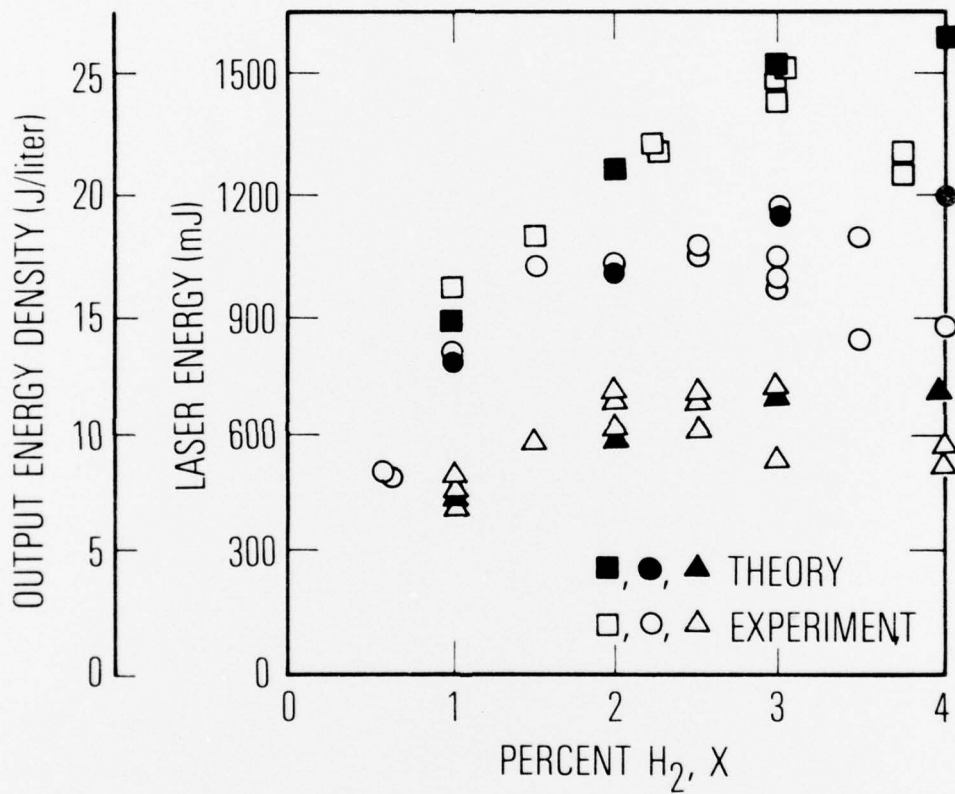


Figure 7. Comparison of Theory and Experimental Results of Hofland et al.<sup>6</sup> at 800 Torr. Note that the calculated and observed pulse duration is 3  $\mu$ sec for the 6 F<sub>2</sub>:3 H<sub>2</sub>:54 He:37 Ar mixture. For cases with Ar, the value of (F + H)/(F<sub>2</sub>) used in the model is 0.009 and 0.006 for cases with [He] = 36 and 54, respectively, and 0.005 for the case without Ar. C<sub>op</sub>% is the percent transmitted by the output coupler.

## V. CONCLUSIONS

A simplified model of the  $H_2 + F_2$  pulsed chemical laser has been presented. This model yields results in agreement with a more comprehensive model at about 1% of the cost. Therefore, we expect this model to be the logical tool for use in improving the agreement between theory and experiment. Once this is done, we can then return to the more detailed calculations of the comprehensive model (RESALE) or of the model given in Ref. 14.

In addition, the economy of making accurate theoretical predictions will permit the model to be used extensively in parametric studies or as a "building-block" for incorporation into other models for examining effects of mode structure or other physical phenomena, such as plasma kinetics, on the performance of laser systems.

## APPENDIX A

The detailed chemical kinetic model used for this study is presented here. The rate coefficients given in Table I are based on the review of the rate measurements and predictions given by Cohen.<sup>22</sup> The entire kinetic model was used for the calculations with the comprehensive model (RESALE) presented in this report. Only the appropriate reactions and rate coefficients were used in the simple model.

## APPENDIX B

The Voigt profile at line center is given by<sup>9</sup>

$$\phi(\nu, J) = \left(\frac{\ln 2}{\pi}\right)^{1/2} e^{y^2} [1 - \operatorname{erf}(y)] / \alpha_{DP}(\nu, J) \quad , \quad (B1)$$

where

$$y = (\ln 2)^{1/2} \alpha_{LR} / \alpha_{DP}(\nu, J) \quad . \quad (B2)$$

The Doppler half-half width is

$$\alpha_{DP}(\nu, J) = \left(\frac{2 \times 10^7 N_A kT \ln 2}{W^*}\right)^{1/2} \times \frac{w(\nu, J)}{c} \quad , \quad (B3)$$

and the Lorentz half-half width is

$$\alpha_{LR} = \sum_i [N_i] RT^{1/2} W \sum_j a_j [N_j] / \rho \quad , \quad (B4)$$

where  $\rho$  is the density,  $W^*$  is the molecular weight of HF, and  $W$  is the molecular weight of the total mixture. Only billiard-ball collisions have been included in Eq. (B4).

## REFERENCES

1. R. L. Kerber, A. Ching, M. L. Lundquist, and J. S. Whittier, "An Efficiently Initiated Pulsed  $H_2+F_2$  Laser," IEEE J. Quantum Electron. QE-9, 607 (1973); also, J. S. Whittier and R. L. Kerber, "Performance of an HF Chain-Reaction Laser with High Initiation Efficiency," IEEE J. Quantum Electron. QE-10, 844 (1974).
2. J. V. Parker and R. R. Stephens, "Pulsed HF Chemical Laser With High Electrical Efficiency," Appl. Phys. Lett. 22, 450 (1973).
3. J. Wilson, H. L. Chen, W. Fyfe, R. L. Taylor, R. Little, and R. Lowell, "Electron Beam Dissociation of Fluorine," J. Appl. Phys. 44, 5447 (1973).
4. R. Aprahamian, J. H. S. Wang, J. A. Betts, and R. W. Barth, "Pulse Electron-Beam-Initiated Chemical Laser Operating on the  $H_2/F_2$  Chain Reaction," Appl. Phys. Lett. 24, 239 (1974).
5. R. Hofland, M. L. Lundquist, A. Ching, and J. S. Whittier, "Electron-Beam-Irradiated Discharges Considered for Initiating High-Pressure Pulsed Chemical Lasers," J. Appl. Phys. 45, 2207 (1974).
6. R. Hofland, A. Ching, M. L. Lundquist, and J. S. Whittier, "Atmospheric-Pressure  $H_2-F_2$  Laser Initiated by Electron-Beam Irradiated Discharge," abstract published in IEEE J. Quantum Electron QE-10, 781 (1974); also, TR-0075(5240-50)-3, The Aerospace Corp., El Segundo, Calif. (15 July 1974).
7. N. R. Greiner, L. S. Blair, E. L. Patterson, and R. A. Gerber, "A 100 Gigawatt  $H_2-F_2$  Laser Initiated by an Electron Beam," IEEE J. Quantum. Electron. QE-10, 780 (1974).
8. G. Emanuel, "Analytic Model for a Continuous Chemical Laser," J. Quant. Spectrosc. Radiat. Transfer 11, 1481 (1971).
9. G. Emanuel, W. D. Adams, and E. B. Turner, RESALE-1: A Chemical Laser Computer Program, TR-0172(2776)-1, The Aerospace Corp., El Segundo, Calif. (31 March 1972).
10. R. L. Kerber, G. Emanuel, and J. S. Whittier, "Computer Modeling and Parametric Study for a Pulsed  $H_2+F_2$  Laser," Appl. Opt. 11, 1112 (1972).

11. S. N. Suchard, R. L. Kerber, G. Emanuel, and J. S. Whittier, "Effect of  $H_2$  Pressure on Pulsed  $H_2+F_2$  Laser, Experiment and Theory," J. Chem. Phys. 57, 5065 (1972).
12. A. N. Chester and L. D. Hess, "Study of the HF Chemical Laser by Pulsed-Delay Measurements," IEEE J. Quantum Electron. QE-8, 1 (1972).
13. R. Hofland, D. Sutton, and J. S. Whittier, The Aerospace Corp., El Segundo, Calif., private communication (1974).
14. J. J. T. Hough and R. L. Kerber, "Effect of Cavity Transients and Rotational Relaxation on the Performance of Pulsed HF Chemical Lasers: A Theoretical Investigation," Appl. Opt. 14, 2960 (1975).
15. J. B. Moreno, "Computer Model for the  $H_2+F_2$  Super-Radiant Laser," presented at AIAA 13th Aerospace Sciences Meeting, Pasadena, Calif. (1975).
16. J. R. Creighton and R. K. Pearson, "Calculation of Rotational Non-Equilibrium in a Pulsed HF Laser," presented at 4th Conf. on Chemical and Molecular Lasers, St. Louis, Mo. (1974).
17. J. F. Skifstad, "Theory of an HF Chemical Laser," Combust. Sci. Tech. 6, 287 (1972).
18. R. L. Kerber, "Simple Model of a Line Selected, Long Chain, Pulsed DF-CO<sub>2</sub> Chemical Transfer Laser," Appl. Opt. 12, 1157 (1973).
19. G. Emanuel and J. S. Whittier, "Closed-form Solution to Rate Equations for an F+H<sub>2</sub> Laser Oscillator," Appl. Opt. 11, 2047 (1972).
20. It was found that significant error would result if the characteristic rotational temperature  $\theta_r$  was taken as a constant value independent of the vibrational level  $v$ . When this was corrected, significant improvement was observed in the comparison with the comprehensive model.
21. M. A. Kwok, Aerospace Corp., Los Angeles, Calif., private communication (1975).
22. N. Cohen, A Review of Rate Coefficients for Reactions in the  $H_2-F_2$  Laser System, TR-0073(3430)-9, The Aerospace Corp., El Segundo, Calif. (1 November 1972).

## THE IVAN A. GETTING LABORATORIES

The Laboratory Operations of The Aerospace Corporation is conducting experimental and theoretical investigations necessary for the evaluation and application of scientific advances to new military concepts and systems. Versatility and flexibility have been developed to a high degree by the laboratory personnel in dealing with the many problems encountered in the nation's rapidly developing space and missile systems. Expertise in the latest scientific developments is vital to the accomplishment of tasks related to these problems. The laboratories that contribute to this research are:

Aerophysics Laboratory: Launch and reentry aerodynamics, heat transfer, reentry physics, chemical kinetics, structural mechanics, flight dynamics, atmospheric pollution, and high-power gas lasers.

Chemistry and Physics Laboratory: Atmospheric reactions and atmospheric optics, chemical reactions in polluted atmospheres, chemical reactions of excited species in rocket plumes, chemical thermodynamics, plasma and laser-induced reactions, laser chemistry, propulsion chemistry, space vacuum and radiation effects on materials, lubrication and surface phenomena, photo-sensitive materials and sensors, high precision laser ranging, and the application of physics and chemistry to problems of law enforcement and biomedicine.

Electronics Research Laboratory: Electromagnetic theory, devices, and propagation phenomena, including plasma electromagnetics; quantum electronics, lasers, and electro-optics; communication sciences, applied electronics, semi-conducting, superconducting, and crystal device physics, optical and acoustical imaging; atmospheric pollution; millimeter wave and far-infrared technology.

Materials Sciences Laboratory: Development of new materials; metal matrix composites and new forms of carbon; test and evaluation of graphite and ceramics in reentry; spacecraft materials and electronic components in nuclear weapons environment; application of fracture mechanics to stress corrosion and fatigue-induced fractures in structural metals.

Space Sciences Laboratory: Atmospheric and ionospheric physics, radiation from the atmosphere, density and composition of the atmosphere, aurorae and airglow; magnetospheric physics, cosmic rays, generation and propagation of plasma waves in the magnetosphere; solar physics, studies of solar magnetic fields; space astronomy, x-ray astronomy; the effects of nuclear explosions, magnetic storms, and solar activity on the earth's atmosphere, ionosphere, and magnetosphere; the effects of optical, electromagnetic, and particulate radiations in space on space systems.

THE AEROSPACE CORPORATION  
El Segundo, California